Petroleum Science
https://doi.org/10.1007/s12182-020-00500-7

ORIGINAL PAPER

Hydrocracking diversity in *n*-dodecane isomerization on Pt/ZSM-22 and Pt/ZSM-23 catalysts and their catalytic performance for hydrodewaxing of lube base oil

Shan-Bin Gao[1,2] · Zhen Zhao[1] · Xue-Feng Lu[2] · Ke-Bin Chi[2] · Ai-Jun Duan[1] · Yan-Feng Liu[2] · Xiang-Bin Meng[2] · Ming-Wei Tan[2] · Hong-Yue Yu[2] · Yu-Ge Shen[2] · Meng-Chen Li[2]

Received: 21 April 2020
© The Author(s) 2020

Abstract
Nobel metallic Pt/ZSM-22 and Pt/ZSM-23 catalysts were prepared for hydroisomerization of normal dodecane and hydrodewaxing of heavy waxy lube base oil. The hydroisomerization performance of n-dodecane indicated that the Pt/ZSM-23 catalyst preferred to crack the C–C bond near the middle of *n*-dodecane chain, while the Pt/ZSM-22 catalyst was favorable for breaking the carbon chain near the end of *n*-dodecane. As a result, more than 2% of light products (gas plus naphtha) and 3% more of heavy lube base oil with low-pour point and high viscosity index were produced on Pt/ZSM-22 than those on Pt/ZSM-23 while using the heavy waxy vacuum distillate oil as feedstock.

Keywords Isomerization · Hydrocracking · Catalysts · Pt/ZSM-22 · Pt/ZSM-23 · Dodecane · Lube base oil

1 Introduction

Hydroisomerization of long-chain hydrocarbons (normal-paraffins) to branched isomers (isoparaffins) plays an essential role in many processes in the petroleum refining industry (Gerasimov et al. 2013; Liu et al. 2009). Hydroisomerization of C_4–C_7 hydrocarbons could produce gasoline with a high octane number (Liu et al. 2011; Buluchevskii et al. 2018), while isomerization of C_7–C_{15} paraffins could be applied to manufacture diesel fuel with high cetane numbers and improved cold flow properties (Rüfer and Reschetilowski 2012; Blomsma et al. 1997). Furthermore, the isomerization of *n*-paraffins heavier than C_{15} can be employed to obtain lube oils with a high viscosity index to ensure volatility and cold flow properties for automotive engine lubricants (Park and Ihm 2000; Zhang et al. 2001). It is well known that the selectivity of paraffin isomerization depends primarily on the balance between the acid and metal catalyst functions (Galperin 2001). Coonradt and Garwood (1964) presented the classical bifunctional hydro-conversion mechanism of alkanes on bifunctional acid-metal catalysts. Tian et al. (2009) developed a new di-tetrahedron matrix on isomerization reaction of long *n*-alkanes based on the traditional bi-functional matrix. Generally, shape-selectivity, acidity, and metal function should be combined synergestically to predict the selectivity and activity of catalysts in the dewaxing reaction of lubricant base oil. Therefore, it is necessary to develop ideal bifunctional catalysts with high selectivity for hydroisomerization of long-chain hydrocarbons to the aimed products. In particular, the shape selection of molecular sieve channel should be strengthened.

Considerable efforts have been targeted at the preparation of bifunctional catalysts containing metallic sites for hydrogenation/dehydrogenation and acid sites for skeletal isomerization (Gong et al. 2012; Yang et al. 2012). Molecular sieves with suitable acid sites, such as ZSM-12 (Gopal and Smirniotis 2003), ZSM-22 (Wang et al. 2020), mordenite (Chica and Corma 1999), Y-zeolite (Lee et al. 2013), L-zeolite (Zhang and Smirniotis 1999), and silicoaluminophosphates (SAPO-n) (Hochtl et al. 2000; Ren et al. 2006; Wang et al. 2003), have been studied extensively for hydroisomerization reactions. Particularly, the acidity and channel structure of molecular sieves have great influences

Edited by Xiu-Qiu Peng

✉ Zhen Zhao
zhenzhao@cup.edu.cn

[1] State Key Laboratory of Heavy Oil Processing, China University of Petroleum, Beijing 102249, China

[2] Petrochemical Research Institute, PetroChina Company Limited, Beijing 100195, China

Published online: 04 September 2020

on the product selectivity of hydroisomerization reactions (Zhang et al. 1998). Wang et al. (2008) studied the effect of the acidity of ZSM-22 on its catalytic performance for hydroisomerization of *n*-dodecane. The results suggested that high conversion, high iso-dodecane selectivity, and low cracking were achieved for Pt/ZSM-22 catalyst treated by the combination of NH_4^+ ion-exchange and $(NH_4)_2SiF_6$. The catalyst with Brønsted acid sites of medium strength was more suitable for the hydroisomerization of *n*-dodecane. In addition, Lee and Ihm (2013) reported that magnesium promoter resulted in the changes of acidity and dispersion of Pt metals. The magnesium-promoted Pt/ZSM-23 exhibited better hydroisomerization selectivity of *n*-hexadecane compared with Pt/ZSM-22. The previous research proved that not only the selectivity in hydroisomerization of *n*-octane was highly influenced by the channel structure of molecular sieves, but also the conversion of *n*-octane was dependent on the acidity of molecular sieves (Hu et al. 2005). Monodimensional medium-pore molecular sieves would be the ideal catalytic materials for higher isomerization selectivity in hydroisomerization of *n*-octane regardless of acid strength, such as ZSM-22 and ZSM-23. Chen et al. (2018a, b) synthesized a series of Fe-substituted ZSM-23 with different Fe contents, and the Pt/Fe-substituted catalysts showed lower activity to the hydroisomerization of *n*-hexadecane, while it gave higher isomerization selectivity. Highly crystallized ZSM-23 zeolite which synthesized by pyrrolidine and isopropylamine and the bifunctional catalysts showed excellent catalytic performance (Chen et al. 2018a, b). They (Chen et al. 2017) also reported the seed-assisted synthesis of ZSM-23 zeolite in the absence of alkali metal ions, and that the catalyst possesses an appropriate acid site distribution and smaller crystal size. Isohexadecane selectivity reached 60% at 75% conversion of *n*-hexadecane in the reaction of *n*-hexadecane hydroisomerization. However, for one-dimensional channel molecular sieves such as ZSM-22 and ZSM-23, the reported research works are more about the modification of materials, and the performance of hydroisomerization, but less research work on the shape selectivity of hydrocracking in the process of hydroisomerization (Zhang et al. 2016). As we know, the cracking reaction is inevitable in the process of hydroisomerization, the performance of hydroisomerization affects the properties of products, and the cracking performance influences the distribution of products. Therefore, it is significant to study the hydrocracking performance of different molecular sieves in the process of hydroisomerization and to realize the desirable hydroisomerization and controllable cracking of the catalyst.

In this work, two systems of Pt/ZSM-22 and Pt/ZSM-23 catalysts with different SiO_2/Al_2O_3 ratios were prepared. Hydroisomerization of *n*-dodecane, i.e., using *n*-dodecane as the feedstock of model reaction for *n*-paraffin dewaxing, was performed over the above two bifunctional catalysts. Interestingly, the diversity of hydrocracking behavior in hydroisomerization reaction is discussed in detail. Moreover, the reaction behaviors over both catalysts with heavy waxy vacuum distillate oil as the feedstock are analyzed systematically.

2 Experimental

2.1 Preparation of catalysts

ZSM-22 and ZSM-23 zeolites with different SiO_2/Al_2O_3 ratios were hydrothermally synthesized in Teflon-lined stainless-steel autoclaves (Wang et al. 2008). ZSM-22 and ZSM-23 were prepared by using the methods in US patents (Ernest and Valyocsik 1984a, b). The as-synthesized ZSM-22 and ZSM-23 zeolites were calcined at 550 °C for 5 h under static air to remove the organic template. These two zeolites were separately mixed with pseudoboehmite (zeolite/pseudoboehmite = 7:3, wt/wt) and nitric acid. Then, the two mixtures were extruded accordingly to obtain the composite supporters. Certain quantity of Pt was then loaded on each composite support by impregnation with an aqueous solution of $H_2PtCl_6{\cdot}6H_2O$. After dried at 120 °C for 8 h and calcined at 480 °C for 4 h, ZSM-22 and ZSM-23 molecular sieves with different SiO_2/Al_2O_3 ratios were impregnated with the same content of Pt to prepare a series of hydroisomerization catalysts.

2.2 Characterization of catalysts

Powder X-ray diffraction (PXRD) patterns of the catalysts were recorded on a PANalyticalX´Pert PRO diffractometer using Cu Kα radiation at 40 kV and 40 mA. Chemical compositions were measured by a Philips Magix X-ray fluorescence (XRF) spectrometer. BET specific surface area, pore volumes, adsorption–desorption curves, and median micropore size were measured by a Micromeritics ASAP-2460 physical analyzer by N_2 adsorption at − 196 °C. The acidity of catalysts was tested by temperature-programmed desorption of ammonia (NH_3-TPD), with 0.1 g ZSM-22 or 0.1 g ZSM-23 heated at 450 °C for 2 h under helium with a flow rate of 40 mL/min. After the temperature fell down to 100 °C, NH_3 was introduced until saturation. After helium purged for 30 min, NH_3 was desorbed by increasing temperature to 700 °C at a rate of 20 °C/min. Desorption ammonia was detected by a TCD detector. Scanning electron microscopy (SEM) analyses were performed to determine the crystallite size and morphology. A JSM6360LA scanning electron microscope was used with a voltage of 20 kV.

2.3 Catalytic performance measurements

Before catalytic test, the catalysts were reduced under H_2 with a flow rate of 200 mL/min. The reaction conditions are as follows, H_2 partial pressure of 0.1 MPa, the reaction temperature of 250 °C for 1 h and 350 °C for 1 h in the heating rate of 5 °C/min from room temperature.

Isomerization of microreactor-GC tests was conducted in a tubular consecutive down-flow fixed bed tube reactor. 2 mL of each catalyst was loaded in the middle zone of reactor. Martens et al. (1989, 2001) proposed that the chain length of the *n*-paraffin influenced the isomer distribution of the product. All carbenium ion reactions occur at constant rates when the chain lengths of the feed paraffins are larger than nonane. Therefore, we chose *n*-dodecane as the probe molecule to study the performance of isomerization and cracking on Pt/ZSM-22 and Pt/ZSM-23 in this study. The purity of feedstock *n*-dodecane is more than 99%. The reaction conditions were as follows, liquid hourly space velocity (LHSV) of 1.0 h^{-1}, H_2/*n*-dodecane molar ratio of 2.0 mol/mol, H_2 pressure of 7.0 MPa, and the reaction temperature within the range of 270–370 °C. All products were separated into gas phase product and liquid phase product by a high pressure separator. Gas phase products were analyzed by an on-line GC-FID/TCD. The HP-PLOT Al_2O_3 column was used. Liquid phase products were condensed and collected in a tank at room temperature for off-line analysis by a GC-FID. The length and thickness of GC capillary column were 50 m and 1.31 μm, respectively. Its internal diameter is 0.32 mm. At the same time, a CP-Sil-5CB stationary phase was used.

Pilot tests of paraffin base heavy waxy oil were performed in a down-flow fixed bed tube reactor equipment. 200 mL Pt/ZSM-22 and 200 mL Pt/ZSM-23 catalysts are loaded in two fixed tube reactors, respectively. Heavy waxy oil with pour point of 63 °C was taken as the feedstock. The operating conditions are as follows, hydrogen partial pressure 13.0 MPa, H_2/oil volume ratio 600 Nm^3/m^3, and LHSV 1.0 h^{-1}. The reaction temperatures were varied to make sure that the pour points of the heavy products should be lower than − 15 °C. All products were separated into gas phase product and liquid phase product. Liquid phase product should be distilled to light cut (boiling range of 180 °C^-), middle cut (boiling range of 180–420 °C), and heavy cut (boiling range of 420 °C^+) by true boiling point (TPB) unit. The properties of heavy cut, such as pour point, viscosity, were analyzed by the usual methods.

3 Results and discussion

3.1 Physicochemical properties of ZSM-22 and ZSM-23

ZSM-22 and ZSM-23 possess related zeolite structures of TON and MTT topologies, respectively. The MTT framework can be considered as a recurrently twinned variant of TON framework (Meier et al. 1996). The 10-membered ring pores in both topologies are undulated, but the undulation pattern is different. In materials with MTT topology, the cross section has the shape of a teardrop, with maximum and minimum free diameters of 0.52 and 0.45 nm, respectively. In the TON structure types, the 10-membered ring delineating the pores have an elliptical shape, with maximal and minimal free diameters of 0.57 and 0.46 nm, respectively. Consequently, the architectures of the pores and pore mouths of TON and MTT are substantially different (Huybrechtsa et al. 2005). XRD patterns of ZSM-22 and ZSM-23 samples with

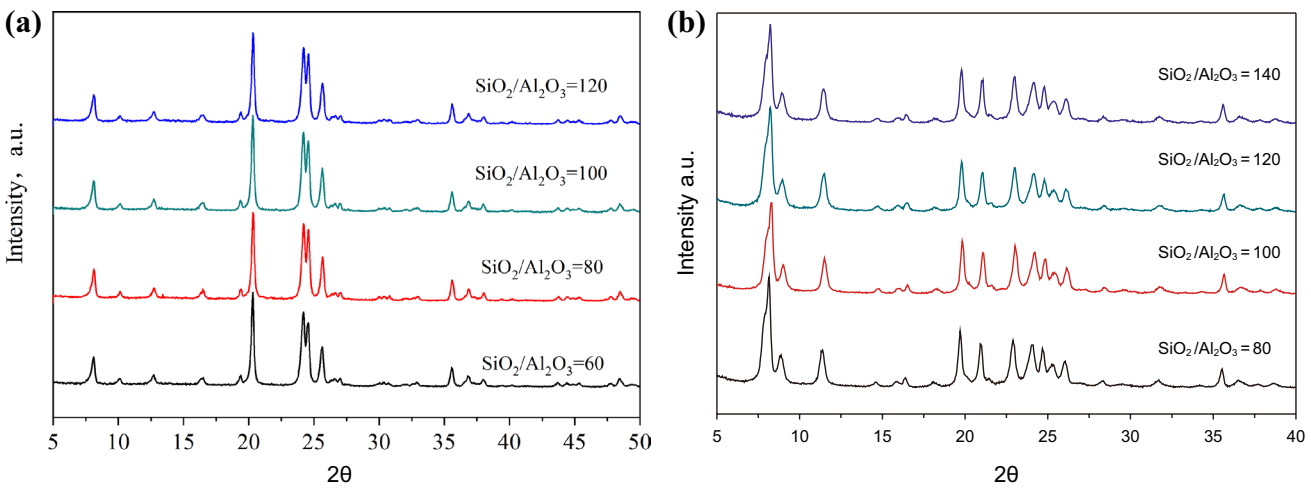

Fig. 1 XRD patterns of ZSM-22 (**a**) and ZSM-23 (**b**)

different SiO_2/Al_2O_3 ratios are shown in Fig. 1, which are in good agreement with those reported in the literature (Fyfe et al. 2005; Ernest and Valyocsik 1984a, b). The SEM images in Fig. 2 showed the perfect crystals of the synthesized ZSM-22 and ZSM-23 zeolites. The lengths of the two crystals are almost the same. The acicular crystals of ZSM-22 and ZSM-23 exhibited their respective appearances, in which ZSM-22 cluster is dense and ZSM-23 cluster is relatively loose.

The surface acid properties of ZSM-22 and ZSM-23 catalysts were investigated by NH_3-TPD (Fig. 3). Both ZSM-22 and ZSM-23 had two ammonia desorption peaks, one centered at around 200 °C and the other one at around 400 °C. The former ammonia desorption peak at low temperature represents weak acid center and the latter one at high temperature ascribes to the strong acid center. For each molecular sieve, with the decreasing of SiO_2/Al_2O_3 ratio, ammonia desorption peak moved to high temperature direction, and the area of ammonia desorption curve becomes larger, which indicate that the same kind of molecular sieve with low SiO_2/Al_2O_3 ratio has more acid content and stronger acid strength. From the NH_3-TPD curves, it can be concluded that for the different molecular sieves, the ZSM-22 and ZSM-23 zeolites with the same SiO_2/Al_2O_3 ratio have different acid properties. The weak and strong acid desorption peaks for ZSM-22 moved from 185 to 198 °C and 380 to 405 °C, respectively, while for ZSM-23 sample these peaks shifted from 193 to 197 °C and 406 to 415 °C, respectively. Therefore, it is indicated that ZSM-23 exhibits much stronger acidity than ZSM-22.

The FT-IR spectra of pyridine adsorption on the ZSM-22 and ZSM-23 zeolites are shown in Fig. 4. Generally, the pyridine molecules adsorbed on the weak acid sites can desorb at a relatively low temperature of 200 °C, and pyridine molecules adsorbed on strong acid sites desorb at a relatively high temperature of 350 °C. Normally, the IR adsorption band of pyridine at 1447–1460 cm^{-1} can be assigned to the adsorption of pyridine molecules on the Lewis acid sites, and the IR adsorption band of pyridine at 1540 cm^{-1} is ascribed to the adsorption of pyridine molecules on the Brønsted acid sites. The acidity amounts of Brønsted and Lewis acid sites decreased significantly after the two catalysts were degassed

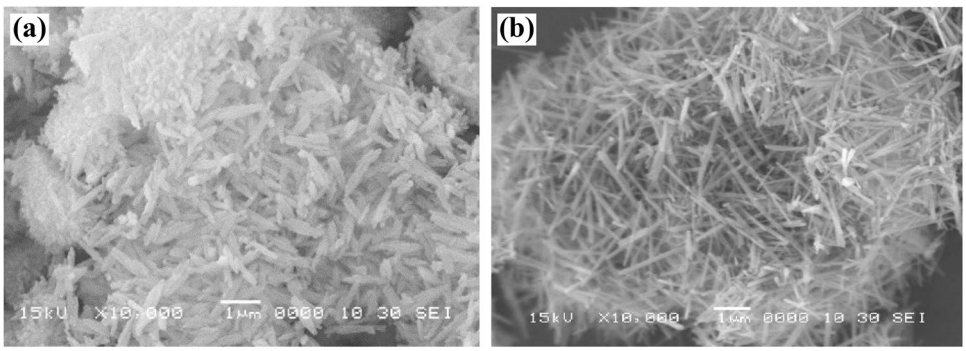

Fig. 2 SEM images of ZSM-22 (**a**) and ZSM-23 (**b**) samples

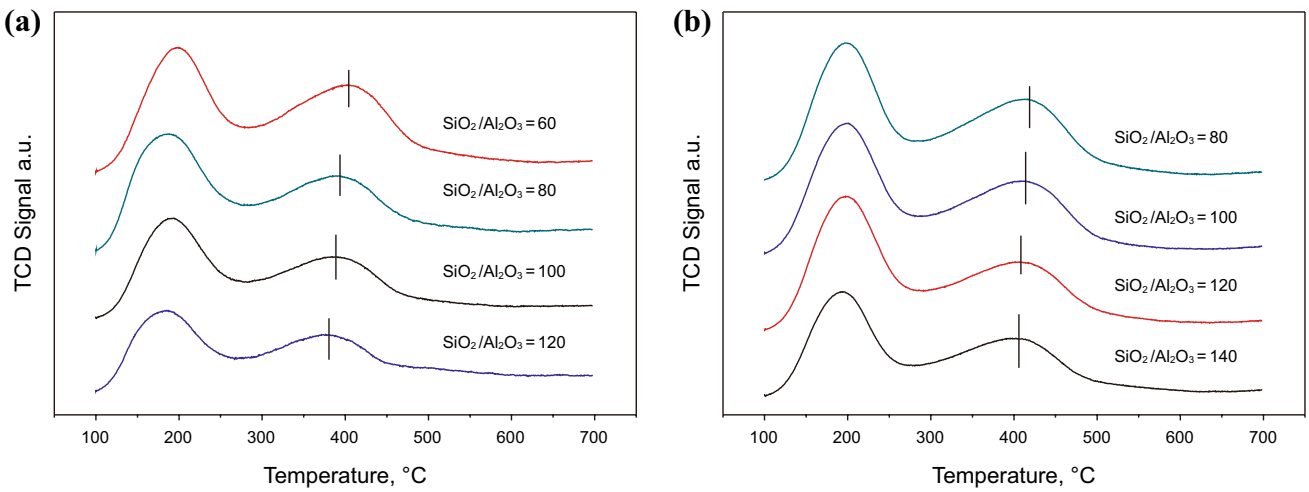

Fig. 3 NH_3-TPD profiles of ZSM-22 (**a**) and ZSM-23 (**b**)

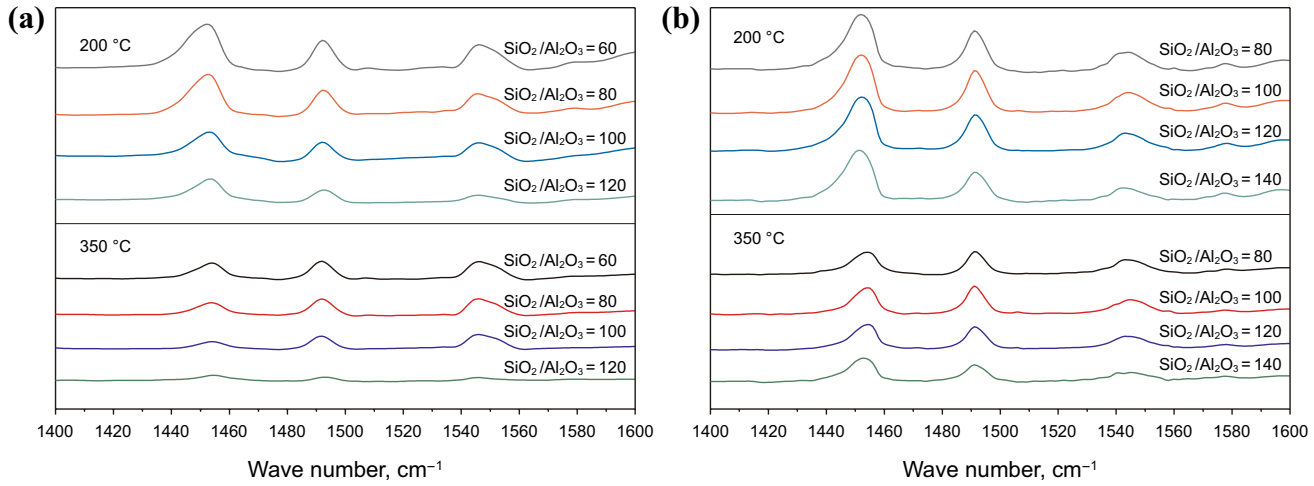

Fig. 4 The FT-IR spectra of pyridine adsorption on ZSM-22 (**a**) and ZSM-23 (**b**) zeolites

from 200 to 350 °C. According to the spectra, the weak acid sites exist in ZSM-22, ZSM-23 obviously, and the contents of Lewis acid sites were greater than Brønsted sites of these two molecular sieves. Although the Brønsted acid sites is favorable for hydroisomerization, cracking reaction is more likely to happen with large amount of Brønsted acid sites, and reducing the ratio of Brønsted and Lewis acid sites is favorable for improving the isomerization selectivity and isomer yield (Fu et al. 2018). At the same time, with the same silica-alumina ratio, the acid content of ZSM-23 was higher than that of ZSM-22, which is consistent with the results of NH_3-TPD.

N_2 adsorption–desorption isotherms were measured to determine the microporous structure. The isotherms of ZSM-22 and ZSM-23 are shown in Fig. 5, and the derived textural properties are listed in Table 1. After fully detemplation, all samples display similar isotherms of typical microporous structure. The total surface areas of ZSM-22 and ZSM-23 are more than 200 m^2/g, and the micropore surface areas of ZSM-22 and ZSM-23 are about 170 m^2/g; meanwhile, the micropore volumes are all about 0.08 mL/g. Furthermore, the median micropore widths are about 0.58 nm for ZSM-22, and about 0.54 nm for ZSM-23. These mean that all the ZSM-22 and the ZSM-23 samples possess the same microporous sizes. Nevertheless, the median micropore width of ZSM-22 is slightly bigger than ZSM-23, which is inconsistent with the theoretical value.

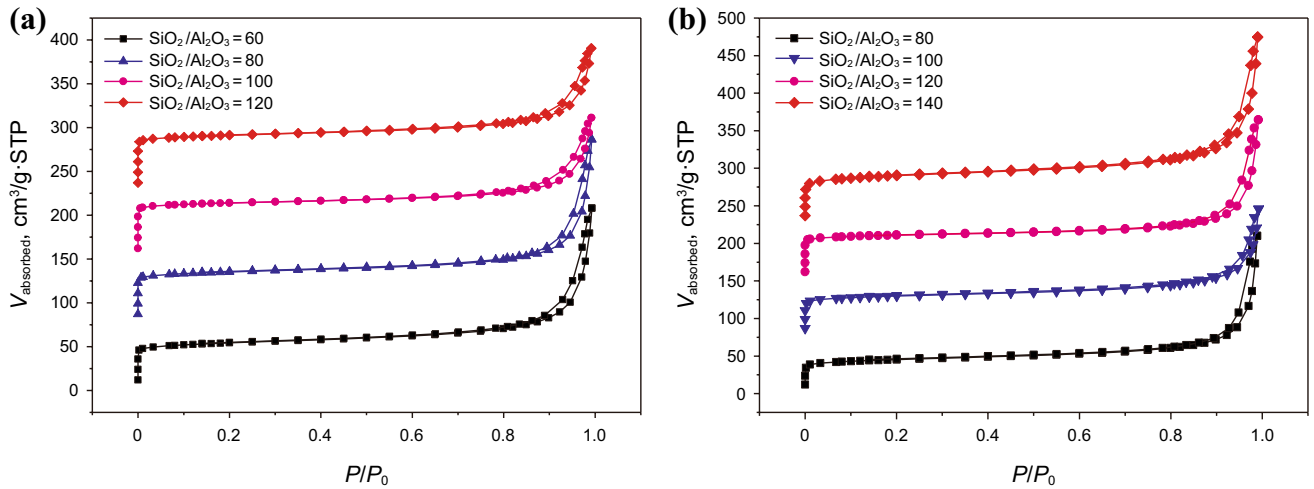

Fig. 5 N_2 adsorption and desorption isotherms of ZSM-22 (**a**) and ZSM-23 (**b**)

Table 1 Textural properties for ZSM-22 and ZSM-23 with different SiO_2/Al_2O_3 ratios

Samples	Surface area, $m^2\ g^{-1}$			Pore volume, $mL\ g^{-1}$			Median pore width
	Total	Micropore	External	Total	Micropore	External	Micropore
ZSM-22-60	201.7	172.4	29.3	0.255	0.085	0.167	0.582
ZSM-22-80	219.7	178.4	30.3	0.247	0.088	0.156	0.591
ZSM-22-100	199.7	167.7	32.0	0.236	0.082	0.151	0.577
ZSM-22-120	205.1	169.4	35.7	0.249	0.083	0.163	0.580
ZSM-23-80	209.2	168.0	41.2	0.203	0.081	0.116	0.532
ZSM-23-100	227.6	168.5	39.1	0.194	0.083	0.106	0.544
ZSM-23-120	235.8	166.8	69.1	0.201	0.082	0.112	0.541
ZSM-23-140	233.2	170.3	62.9	0.198	0.079	0.120	0.542

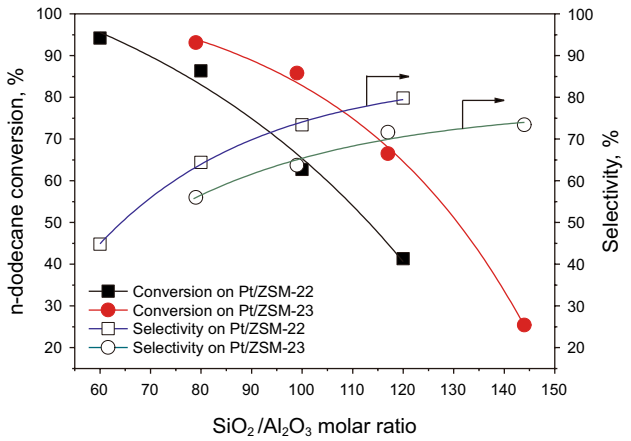

Fig. 6 n-C_{12} conversion and i-C_{12} selectivity on Pt/ZSM-22 and Pt/ZSM-23 with various SiO_2/Al_2O_3 ratios.

3.2 Hydrocracking diversity in the hydroisomerization of *n*-dodecane on Pt/ZSM-22 and Pt/ZSM-23 catalysts

Two systems of Pt/ZSM-22 and Pt/ZSM-23 catalysts with various SiO_2/Al_2O_3 ratios were prepared and tested in a microreactor using n-dodecane as the feedstock. The catalytic performance of these two systems of catalysts is shown in Fig. 6. For each system of the as-prepared catalysts, the conversion of n-dodecane decreases and the selectivity of i-dodecane increases with the increasing of SiO_2/Al_2O_3 ratio. In the SiO_2/Al_2O_3 ratio ranging from 80 to 120, the conversion of n-dodecane over Pt/ZSM-23 is greater than that over Pt/ZSM-22 when their SiO_2/Al_2O_3 ratios are same, while the selectivity of i-dodecane over the former is lower than that over the later. The conversions and the selectivities are similar when Pt/ZSM-22 and Pt/ZSM-23 are in SiO_2/Al_2O_3 ratios of 80 and 100, respectively. The primary physicochemical properties of these samples are similar excluding the SiO_2/Al_2O_3 ratio.

These two systems of catalysts are excellent in producing i-C_{12}. The 64%–69% of i-C_{12} selectivity could be obtained when n-C_{12} conversion achieves 85%–86% over the sample 1 to the sample 4 under the given reaction conditions (Table 2). Gas phase cracked products (C_1–C_6) and liquid phase cracked products including (C_5–C_{11}) are detected by GC analyses (Fig. 7). C_5 and C_6 species exist in liquid phase products as well as gas phase products at room temperature, so they can be detected in the gaseous and liquid products. The distribution of cracked products, either gaseous products or liquid products, on Pt/ZSM-22 is different from those obtained on Pt/ZSM-23. In the gas phase products, much more C_1–C_3 were produced by Pt/ZSM-22. On the contrary, much more C_4–C_6 were manufactured by Pt/ZSM-23. Accordingly, more C_5, and C_6 species could be found on ZSM-23 in the liquid phase products, and more C_7–C_{11} could be obtained on ZSM-22. This phenomenon reveals that Pt/ZSM-23 prefers to catalyze the cracking of the C–C bond close to the middle position of n-dodecane chain. On the contrary, Pt/ZSM-22 is easier to break the C–C bond near the end of dodecane chain. Figure 7 shows the distribution of cracking products on Pt/ZSM-22 and Pt/ZSM-23 with different SiO_2/Al_2O_3 ratios of 80, 100, respectively. Figures 8 and 9 display the distributions of cracking products on Pt/ZSM-22 and Pt/ZSM-23 with the same SiO_2/Al_2O_3 ratio of 80 and 100, respectively. Very similar product distribution patterns are observed in these three figures. It indicates that the product distribution mainly depends on the pore structure of the zeolite and has little relation with the differences in acid properties.

Figures 10 and 11 display the contents of multibranched isomers and terminal monomethyl isomers of i-C_{12} species, respectively, over Pt/ZSM-22 and Pt/ZSM-23 catalysts as a function of n-dodecane conversion. From Fig. 10, it can be seen that the contents of multibranched isomers on the two catalysts enhance with the increasing of n-dodecane conversion, and as shown in Fig. 11, the contents of multibranched isomers on Pt/ ZSM-22 are

Table 2 Characteristics and isomerization performance on different samples with same *n*-dodecane conversions

Property	Catalyst			
	Pt/ZSM-22	Pt/ZSM-22	Pt/ZSM-23	Pt/ZSM-23
SiO_2/Al_2O_3 molar ratio	80	100	80	100
BET, m^2/g	205.4	186.1	191.3	210.2
Pt, wt%	0.505	0.503	0.503	0.501
Reaction temperature, ℃	300	320	275	295
H_2 partial pressure, MPa	7.0	7.0	7.0	7.0
LHSV, h^{-1}	1.0	1.0	1.0	1.0
$H_2/n\text{-}C_{12}$ ratio, mol/mol	2.0	2.0	2.0	2.0
Liquid yield, %	95.1	97.3	96.6	98.5
Yield of C_6–C_{11}, %	27.2	25.6	29.2	28.1
Yield of $i\text{-}C_{12}$, %	58.4	58.9	55.5	56.5
Yield of $n\text{-}C_{12}$, %	14.4	15.5	15.2	14.4
$n\text{-}C_{12}$ Conversion, %	86.3	84.9	85.3	85.8
$i\text{-}C_{12}$ Selectivity, %	64.4	67.5	62.8	64.9

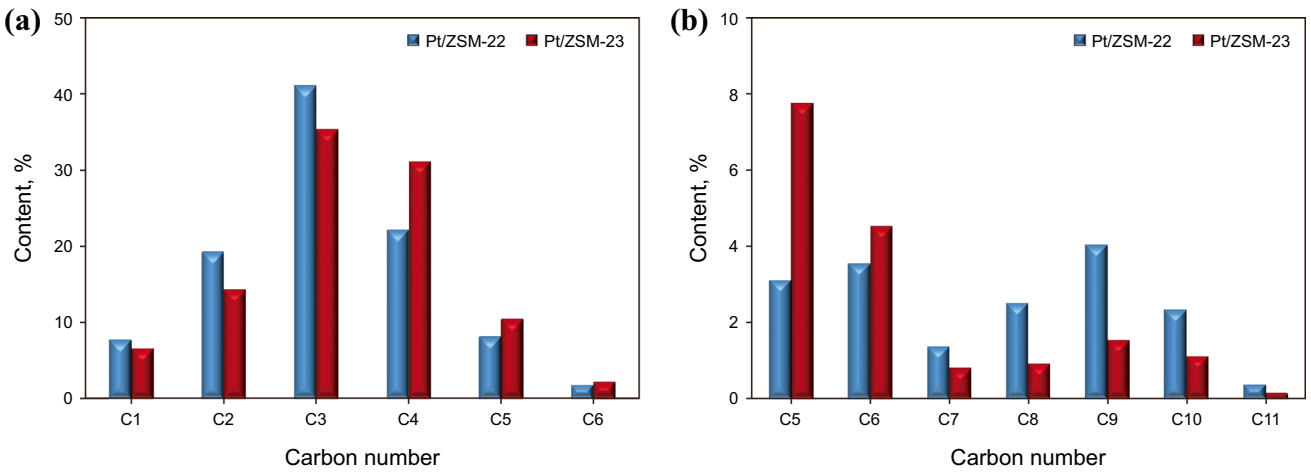

Fig. 7 Distribution of cracking products on Pt/ZSM-22 and Pt/ZSM-23 with different SiO_2/Al_2O_3 ratios of 80 and 100, respectively. **a** Distribution of gas phase cracking products and **b** distribution of liquid phase cracking products

5%–10% higher than those on Pt/ZSM-23. Furthermore, the terminal monomethyl isomers contents on Pt/ ZSM-22 are 5%–10% higher than those on Pt/ ZSM-23, too. Monomethyl isomers with a kinetic diameter of 0.56 nm are more likely to enter into the ZSM-22 channels with a micropore width of 0.57–0.59 nm and then proceed cracking to produce light components. Moreover, they can continue to transform into multibranched isomers, which can be cracked easily. And the terminal monomethyl isomers, which might be easily generated on ZSM-22, will convert into smaller molecules than C_5. However, the intermediate monomethyl isomers, which is easy to be generated on ZSM-23, will transform into C_5, C_6 and other intermediate fractions preferentially.

Figure 12 shows the preference modes for *n*-dodecane cracking on Pt/ZSM-22 and Pt/ZSM-23 catalysts, respectively. Based on the reaction results and product distributions over Pt/ZSM-22 and Pt/ZSM-23 catalysts, the preferable products on Pt/ZSM-22 are $C_{11}+C_1$, $C_{10}+C_2$, and C_9+C_3 as coupled, while ones on Pt/ZSM-23 prefers to produce C_8+C_4, C_7+C_5, and C_6+C_6 as coupled. Martens et al. (1995) proposed a mechanism of pore-mouth and key-lock for hydroisomerization reaction of linear chain *n*-alkanes on bifunctional catalyst. According to Claude and his coworkers' consideration (Claude et al. 2001; Marion and Johan 1999), the pore-mouth mode favors the formation of skeletal branchings at the C_2 and C_3 positions which near to the end of the *n*-alkane chain, while

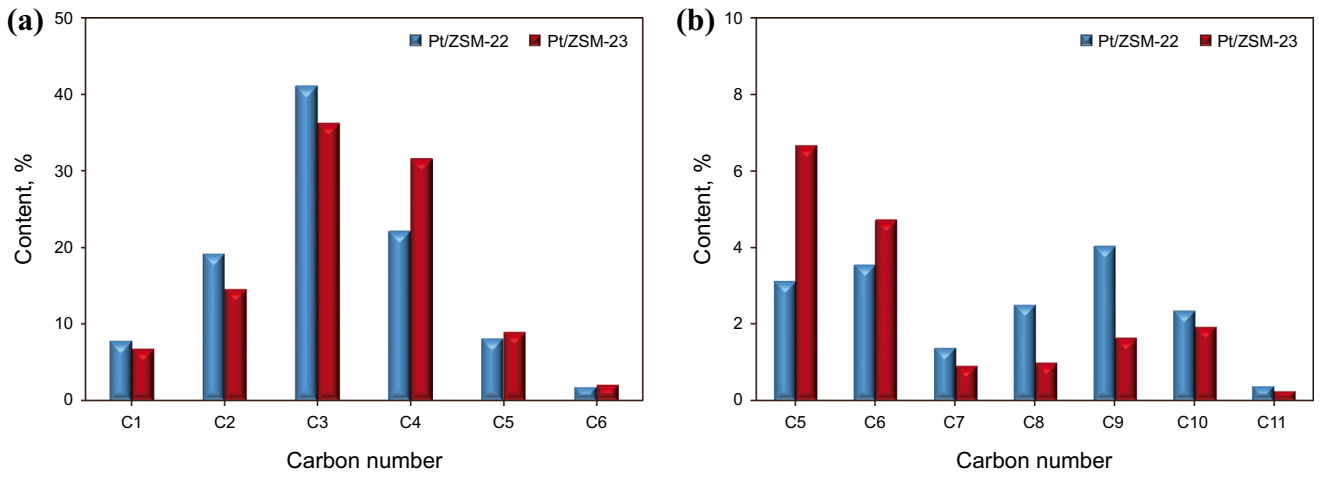

Fig. 8 Distribution of cracking products on Pt/ZSM-22 and Pt/ZSM-23 with the same SiO_2/Al_2O_3 ratio of 80. **a** Distribution of gas phase cracking products and **b** distribution of liquid phase cracking products

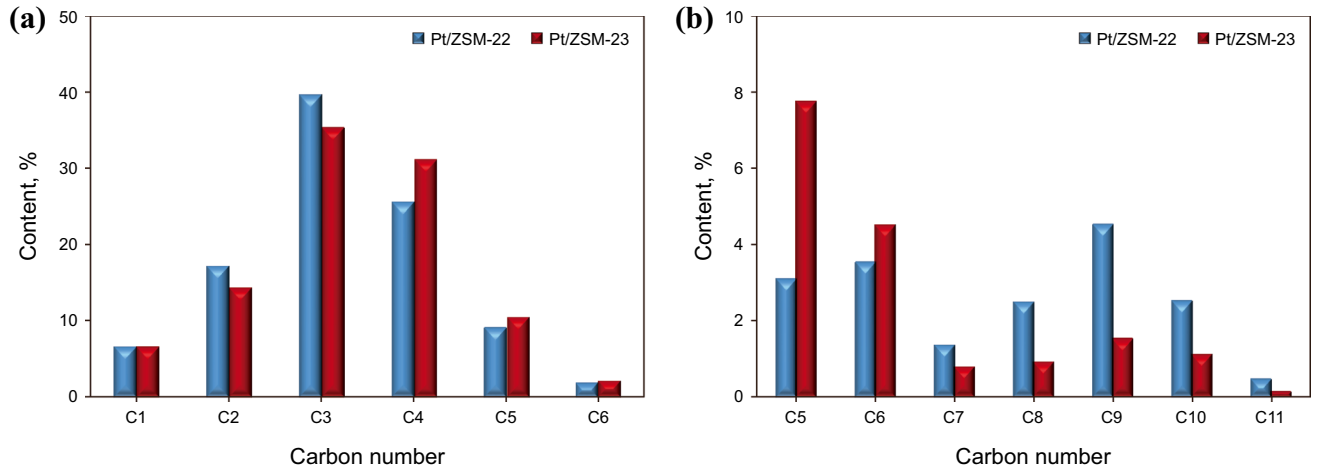

Fig. 9 Distribution of cracking products on Pt/ZSM-22 and Pt/ZSM-23 with the same SiO_2/Al_2O_3 ratio of 100. **a** Distribution of gas phase cracking products and **b** distribution of liquid phase cracking products

the key-lock mode favors the branching at C_5–C_{12} positions in the isomerization process of long *n*-alkanes. Huybrechts et al. (2005) declared that compared to ZSM-22, the preference for branching near the end of the chain is less pronounced on a ZSM-23. The differences between the positional selectivity of methylbranching should be a result of the differences in contributions of pore mouth with respect to key-lock catalysis between ZSM-22 and ZSM-23. The branching selectivities are primarily determined by the framework topology, and much less by the acidity or crystal size. Weitkamp et al. (1983) declared that β-scission of mono-branched alkylcarbenium ions contributed significantly to the mechanism of cleavage. Although ZSM-23 has a little stronger acid contents than ZSM-22, the reaction temperature performed on Pt/ZSM-23 is a little lower than those on Pt/ZSM-22, and the conversions of *n*-C_{12} are almost the same on these two catalysts. We consider that the distribution of cracking and the side products of *n*-alkane isomerization are mainly affected by different positional selectivity of methylbranching on ZSM-22 and ZSM-23 for their different framework topologies, rather than their different acidities. We can also deduce that ZSM-22 favors pore-mouth mode which tends to stimulate the cracking near the end of long-chain alkane, while ZSM-23 is the key-lock mode which trends to lead to cracking near the middle position of *n*-dodecane chain.

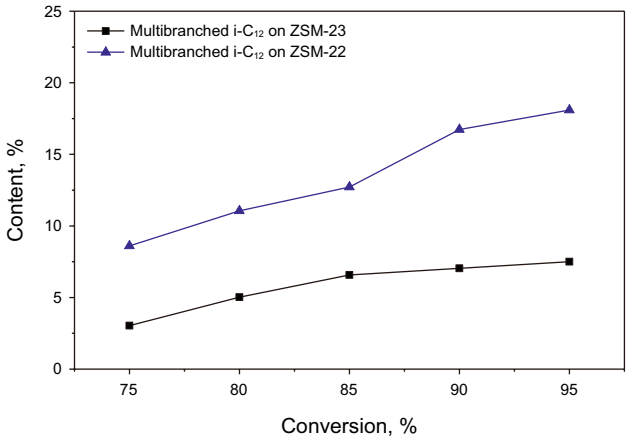

Fig. 10 Content of multibranched isomers as a function of n-dodecane conversion

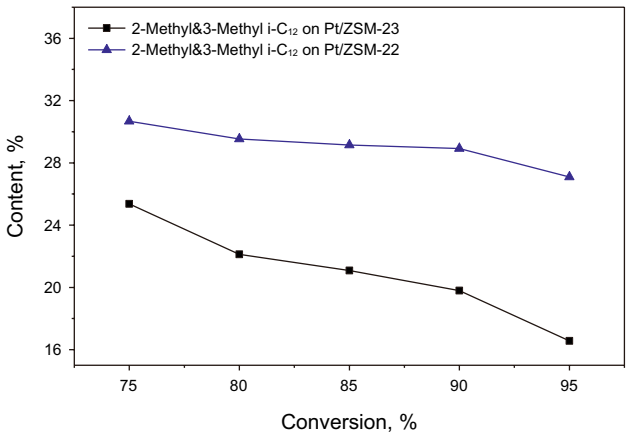

Fig. 11 Content of terminal monomethyl isomers as a function of n-dodecane conversion

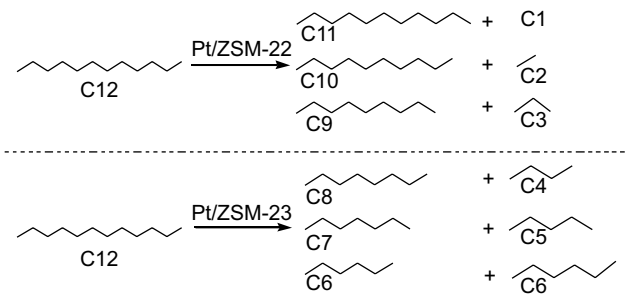

Fig. 12 The preference modes for *n*-dodecane cracking on Pt/ZSM-22 and Pt/ZSM-23 catalysts, respectively

Table 3 Properties of the heavy waxy feedstock

Item	Heavy waxy feedstock
Sulfur content, μg/g	1.2
Nitrogen content, μg/g	1.1
Viscosity, 100 °C, mm^2/s	8.3
Viscosity index[a]	149
Pour point, °C	61
Distillations, °C IBP, 5%, 10%, 30%, 50%, 70%, 90%, 95%, FBP	256, 352, 409, 491, 511, 525, 544, 552, 578

[a]Viscosity index (VI) is an arbitrary measure for the change of viscosity with temperature. VI shows the stability of the viscosity of an oil under temperature change, with values toward + 100 for highly stable, and toward − 100 for highly variable. It is used to characterize lubricating oil in the automotive industry.

3.3 Product distribution in the process for the hydro-dewaxing of waxy lube base oil

The interesting hydrocracking behavior diversity of *n*-dodecane on Pt/ZSM-22 and Pt/ZSM-23 aroused our expectation for a better product distribution on hydroisomerization dewaxing of waxy lube base oil. In general, researchers have to increase the conversion of long-chain *n*-alkanes significantly in order to reduce the pour point to the target value when the pour point of feedstock is extremely high. However, hydrocracking reaction occurs unavoidably following the β-scission mechanism with the increasing of hydroisomerization conversion. Actually, hydrocracking is very effective and necessary in decreasing the pour point of waxy lube base oil. Thus, Pt/ZSM-22 and Pt/ZSM-23 were applied in the hydroisomerization dewaxing of lube base oil. A kind of paraffin-base VGO (vacuum gas oil) after furfural refining with extremely high pour point (61 °C) was used as the feedstock in the hydroisomerization dewaxing on Pt/ZSM-22 and Pt/ZSM-23 (Table 3). The product distributions on both catalysts are shown in Fig. 13. The lube base oil products obtained over Pt/ZSM-22 show good properties in low pour point and high viscosity index, especially for heavy base oil. More light cut (gas and naphtha) product, and more heavy cut (heavy base oil) products are produced, but the middle cut products are relatively less generated on Pt/ZSM-22. This phenomenon corresponds well to the reaction behavior of *n*-dodecane on Pt/ZSM-22. A part of the cracked products has less carbon atoms, while the others have more carbon atoms. The two parts of products were derived from hydrocracking at the end position of the long chain of alkanes. However, the yield of each product on Pt/ZSM-23 increases continuously from light cuts to heavy cuts. More kerosene, diesel, and light base oil but less gas, naphtha and heavy base oil could be obtained on Pt/ZSM-23 than those on Pt/ZSM-22. This is also consistent with

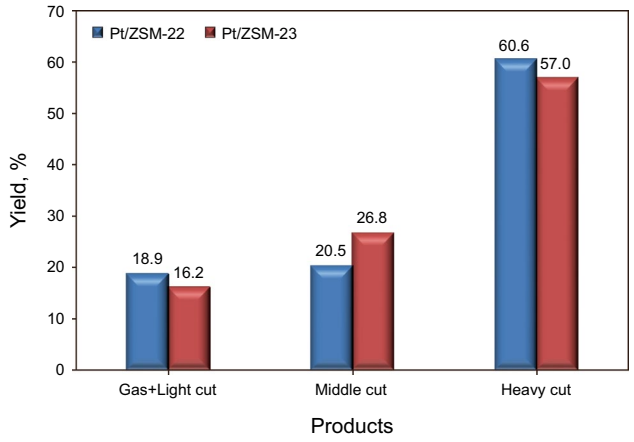

Fig. 13 Product distributions of isomerization dewaxing lube base oil on Pt/ZSM-22 and Pt/ZSM-23 (light cut distillation: 180 °C^{-}, middle cut distillation: 180–421 °C, heavy cut distillation: 421 °C^{+})

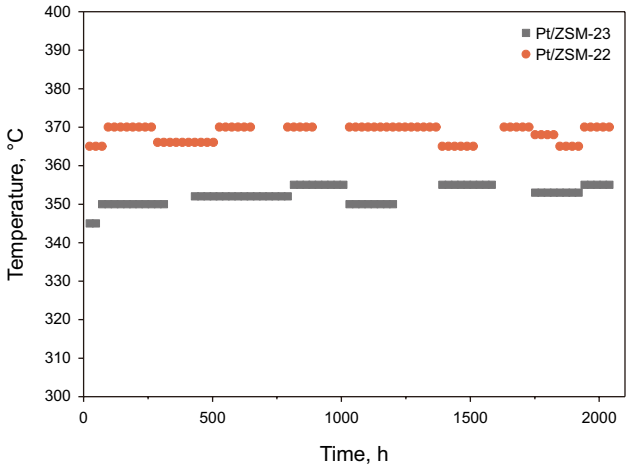

Fig. 14 Long period stability performance of Pt/ZSM-22 and Pt/ZSM-23

the cracking of *n*-dodecane on Pt/ZSM-22 and Pt/ZSM-23. According to Fig. 13, 2.7% more of light products (gas plus naphtha) and 3.6% more of low-pour point heavy lube base oil were produced on Pt/ZSM-22 catalyst than those on Pt/ZSM-23 catalyst. The properties of heavy base oil products on both catalysts are shown in Table 4. The VI values of both base oil can reach above 130. The VI and pour point of the base oil produced on Pt/ ZSM-22 were lower than those on Pt/ZSM-23 because of the formation of more multi-branched isomers. The sulfur content of the products was lower than 1 μg/g. Figure 14 shows the long period stability performance of the both catalysts, and there was no obvious reaction temperature rise when the yield and properties of the base oil were the same in 2000 h. Although some sulfur and nitrogen remained in the feedstocks, the two catalysts showed good impurity resistance and stability.

4 Conclusions

In this work, two systems of microporous ZSM-22 and ZSM-23 zeolites with different SiO_2/Al_2O_3 ratios were prepared, and the corresponding zeolites were loaded with the same content of Pt to prepare a series of hydroisomerization catalysts. The catalytic performance for the isomerization and cracking of *n*-dodecane on Pt/ZSM-22 and Pt/ZSM-23 indicated that the distribution of cracked products, either gas phase products or liquid phase products, was different. In the gas phase products, much more C_1, C_2, C_3 were produced over Pt/ZSM-22. On the contrary, much more C_4, C_5, C_6 were produced over Pt/ZSM-23. Accordingly, in the liquid phase products, more C_5, C_6 could be found on ZSM-23 and more C_7–C_{11} could be obtained on ZSM-22. Because the micropore diameter of ZSM-22 is larger than ZSM-23, so multi-methyl isomers and the terminal monomethyl isomers which can be generated on ZSM-22 easily. While β-scission for Pt/ZSM-23 preferred to crack the C–C bond which was close to the middle position of *n*-dodecane chain. On the contrary, Pt/ZSM-22 was more easy to crack the C–C bond near the end of *n*-dodecane chain. It indicated that the product distribution mainly depends on the pore structure and has little relation with the different acidic properties for the same type topology of zeolite.

One-dimensional channel molecular sieve-supported Pt catalysts were also used in hydroisomerization of lubricating base oil, and the product distribution can be improved through the selection of materials with different pore sizes. More heavy base oil and gas or naphtha were produced on Pt/ZSM-22, and more diesel and light base oil but less gas, naphtha were obtained on Pt/ZSM-23. According to different requirements, it is of great significance to adjust the preparation of catalysts to meet the processing and the product requirements of various feedstocks.

Table 4 Properties of the heavy base oil products

	Heavy base oil on Pt/ZSM-22	Heavy base oil on Pt/ZSM-23
Sulfur content, μg/g	< 1	< 1
Viscosity (100 °C), mm^2/s	10.51	10.22
Viscosity index	130	133
Pour point, °C	-21	-18

Acknowledgements The financial supports by National Key R&D Program of China (Grant No. 2017YFB0306702) are gratefully acknowledged.

Open Access This article is licensed under a Creative Commons Attribution 4.0 International License, which permits use, sharing, adaptation, distribution and reproduction in any medium or format, as long as you give appropriate credit to the original author(s) and the source, provide a link to the Creative Commons licence, and indicate if changes were made. The images or other third party material in this article are included in the article's Creative Commons licence, unless indicated otherwise in a credit line to the material. If material is not included in the article's Creative Commons licence and your intended use is not permitted by statutory regulation or exceeds the permitted use, you will need to obtain permission directly from the copyright holder. To view a copy of this licence, visit http://creativecommons.org/licenses/by/4.0/.

References

Blomsma E, Martens JA, Jacobs PA. Isomerization and hydrocracking of heptane over bimetallic bifunctional PtPd/H-Beta and PtPd/USY zeolite catalysts. J Catal. 1997;165(2):241–8. https://doi.org/10.1006/jcat.1997.1473.

Buluchevskii EA, Fedorova ED, Lavrenov AV, et al. Hydroisomerization of benzene-containing gasoline fraction on Pt/B_2O_3–Al_2O_3 and Pt/WO_3–Al_2O_3 catalysts. Catal Ind. 2018;10:118–25. https://doi.org/10.1134/S2070050418020046.

Chen YJ, Li C, Chen X, et al. Synthesis and characterization of iron-substituted ZSM-23 zeolite catalysts with highly selective hydroisomerization of n-hexadecane. Ind Eng Chem Res. 2018a;57(41):13721–30. https://doi.org/10.1021/acs.iecr.8b03806.

Chen YJ, Li C, Chen X, et al. Synthesis of ZSM-23 zeolite with dual structure directing agents for hydroisomerization of n-hexadecane. Microporous Mesoporous Mater. 2018b;268:216–24. https://doi.org/10.1016/j.micromeso.2018.04.033.

Chen YJ, Li C, Wang L, et al. Seed-assisted synthesis of ZSM-23 zeolites in the absence of alkali metal ions. Microporous Mesoporous Mater. 2017;252:146–53. https://doi.org/10.1016/j.micromeso.2017.06.013.

Chica A, Corma A. Hydroisomerization of pentane, hexane, and heptane for improving the octane number of gasoline. J Catal. 1999;187:167–75. https://doi.org/10.1016/jact.1999.2601.

Claude MC, Vanbutsele G, Martens JA. Dimethyl branching of long n-alkanes in the range from decane to tetracosane on Pt/H–ZSM-22 bifunctional catalyst. J Catal. 2001;203:213–31. https://doi.org/10.1006/jcat.2001.3325.

Coonradt H, Garwood W. Mechanism of hydrocracking reactions of paraffins and olefins. Ind Eng Chem Process Des Dev. 1964;3(1):38–45. https://doi.org/10.1021/i260009a010.

Ernest W, Valyocsik Y. Synthesis of zeolite ZSM-22 with a heterocyclic organic compound. US Patent 4481177 (1984a).

Ernest W, Valyocsik Y. Synthesis of ZSM-23 zeolite. US Patent 4490342 (1984b).

Fu P, Xiao ZR, Liu YH, et al. Support-independent surface functionalization for efficient Pd loading in catalytic hydrogenation. Chemistryselect. 2018;3(11):3351–61. https://doi.org/10.1002/slct.201800106.

Fyfe CA, Kokotailo GT, Strobl H, et al. Correlations between lattice structures of zeolites and their 29Si MAS N.M.R. spectra: zeolites KZ-2, ZSM-12, and Beta. Zeolites. 1988;8(2):132–6. https://doi.org/10.1016/S0144-2449(88)80079-4.

Galperin LB. Hydroisomerization of N-decane in the presence of sulfur and nitrogen compounds. Appl. Catal. A. 2001;209(1–2):257–66. https://doi.org/10.1016/S0926-860X(00)00759-6.

Gerasimov DN, Fadeev VV, Loginova AN, et al. Catalysts based on zeolite ZSM-23 for isodewaxing of a lubricant stock. Catal Ind. 2013;5:123–32. https://doi.org/10.1134/S2070050413020050.

Gong SF, Chen N, Nakayama S, et al. Isomerization of n-alkanes derived from jatrophaoil over bifunctional catalysts. J Mol Catal A Chem. 2013;370:14–211. https://doi.org/10.1016/j.molcata.2012.11.019.

Gopal S, Smirniotis PG. Pt/H-ZSM-12 as a catalyst for the hydroisomerization of C_5–C_7 n-alkanes and simultaneous saturation of benzene. Appl Catal A Gen. 2003;247:113–21. https://doi.org/10.1016/S0926-860X(03)00096-6.

Hochtl M, Jentys A, Vinek H. Hydroisomerization of heptane isomers over Pd/SAPO molecular sieves: influence of the acid and metal site concentration and the transport properties on the activity and selectivity. J Catal. 2000;190:419–27. https://doi.org/10.1016/jact.1999.2761.

Hu YF, Wang XS, Guo XW, et al. Effects of channel structure and acidity of molecular sieves in hydroisomerization of n-octane over bi-functional catalysts. Catal Lett. 2005;100:59–655. https://doi.org/10.1007/s10562-004-3086-9.

Huybrechtsa W, Vanbutselea G, Kristof J, et al. Skeletal isomerization of octadecane on bifunctional ZSM-23 zeolite catalyst. Catal Lett. 2005;100:235–42. https://doi.org/10.1007/s10562-004-3461-6.

Lee SW, Ihm SK. Characteristics of magnesium-promoted Pt/ZSM-23 catalyst for the hydroisomerization of n-hexadecane. Ind Eng Chem Res. 2013;52(44):15359–655. https://doi.org/10.1021/ie400628q.

Lee HW, Jeon JK, Jeong KE, et al. Hydroisomerization of n-dodecane over Pt/Y zeolites with different acid characteristics. Chem Eng J. 2013;232:111–7. https://doi.org/10.1016/j.cej.2013.07.071.

Liu Y, Murata K, Sakanishi K. Hydroisomerization-cracking of gasoline distillate from Fischer–Tropsch synthesis over bifunctional catalysts containing Pt and heteropolyacids. Fuel. 2011;90(10):3056–65. https://doi.org/10.1016/j.fuel.2011.05.004.

Liu P, Zhang X, Yao Y, et al. Pt catalysts supported on β zeolite ion-exchanged with Cr(III) for hydroisomerization of n-heptane. Appl Catal A Gen. 2009;371(1–2):142–7. https://doi.org/10.1016/j.apcata.2009.09.045.

Marion CC, Johan AM. Monomethyl-branching of long n-alkanes in the range from decane to tetracosane on Pt/H-ZSM-22 bifunctional catalyst. J Catal. 2000;190:39–48. https://doi.org/10.1006/jcat.1999.2714.

Martens JA, Souverijns W, Verrelst W, et al. Selective isomerization of hydrocarbon chains on external surfaces of zeolite crystals. Angew Chem Int Ed Engl. 1995;34(22):2528–30. https://doi.org/10.1002/anie.199525281.

Martens JA, Tielen M, Jacobs PA. Relation between paraffin isomerisation capability and pore architecture of large-pore bifunctional zeolites. Stud Surf Sci Catal. 1989;46:49–60. https://doi.org/10.1016/S0167-2991(08)60966-0.

Martens JA, Vanbutsele G, Jacobs PA, et al. Evidences for pore mouth and key-lock catalysis in hydroisomerization of long n-alkanes over 10-ring tubular pore bifunctional zeolites. Catal Today. 2001;65(2–4):111–6. https://doi.org/10.1016/S0920-5861(00)00577-0.

Meier WM, Olson DH, Baerlocher C. Atlas of zeolite structure types. 4th ed. Boston: Elsevier; 1996. p. 8.

Park KC, Ihm SK. Comparison of Pt/zeolite catalysts for n-hexadecane hydroisomerization. Appl Catal A Gen. 2000;203(2):201–9. https://doi.org/10.1016/S0926-860X(00)00490-7.

Ren XT, Li N, Cao JQ, et al. Hydroisomerization of n-decane over Pt/SAPO-41 catalyst. ACS Omega. 2006;298:144–51. https://doi.org/10.1016/j.apcata.2005.09.031.

Rüfer A, Reschetilowski W. Application of design of experiments in heterogeneous catalysis: using the isomerization of n-decane for a parameter screening. Chem Eng Sci. 2012;75:364–75. https://doi.org/10.1016/j.ces.2012.04.002.

Tian Z, Liang D, Lin L. Research and development of hydroisomerization and hydrocracking catalysts in Dalian Institute of Chemical Physics. Chin J Catal. 2009;30(8):705–10. https://doi.org/10.1016/S1872-2067(08)60120-5.

Wang LJ, Guo CW, Yan SR, et al. High-silica SAPO-5 with preferred orientation: synthesis, characterization and catalytic applications. Microporous Mesoporous Mater. 2003;64:63–72. https://doi.org/10.1016/S1387-1811(03)00482-7.

Wang G, Liu QJ, Su WG, et al. Hydroisomerization activity and selectivity of n-dodecane over modified Pt/ZSM-22 catalysts. Appl Catal A Gen. 2008;335:20–7. https://doi.org/10.1016/j.apcata.2007.11.002.

Wang XY, Zhang XW, Wang QF. N-dodecane hydroisomerization over Pt/ZSM-22: controllable microporous Brönsted acidity distribution and shape-selectivity. Appl Catal A Gen. 2020. https://doi.org/10.1016/j.apcata.2019.117335.

Weitkamp J, Jacobs PA, Martens JA. Isomerization and hydrocracking of C_9 through C_{16} n-alkanes on Pt/HZSM-5 zeolite. Appl Catal. 1983;8(1):123–41. https://doi.org/10.1016/0166-9834(83)80058-X.

Yang J, Kikhtyanin OV, Wu W, et al. Influence of the template on the properties of SAPO-31 and performance of Pd-loaded catalysts for n-paraffin isomerization. Microporous Mesoporous Mater. 2012;150:14–24. https://doi.org/10.1016/micromeso.2011.09.020.

Zhang S, Chen SL, Dong P, et al. Characterization and hydroisomerization performance of SAPO-11 molecular sieves synthesized in different media. Appl Catal A Gen. 2007;332(1):46–55. https://doi.org/10.1016/j.apcata.2007.07.047.

Zhang M, Chen YJ, Liang CH, et al. Shape selectivity in the conversion of hexadecane to iso-hexadecane over 10-ring zeolites: ZSM-22, ZSM-23, ZSM-35 and ZSM-48. Ind Eng Chem Res. 2016;55:6069–78. https://doi.org/10.1021/acs.iecr.6b01163.

Zhang W, Smirniotis P. Effect of zeolite structure and acidity on the product selectivity and reaction mechanism forn-octane hydroisomerization and hydrocracking. J Catal. 1999;182:400–16. https://doi.org/10.1016/jact.1999.2337.